



Society of Petroleum Engineers

SPE-197208-MS

Practical Application of Tensor Model in Laminated Sand Shale Analysis

Aditya Ariewijaya, Halliburton

Copyright 2019, Society of Petroleum Engineers

This paper was prepared for presentation at the Abu Dhabi International Petroleum Exhibition & Conference held in Abu Dhabi, UAE, 11-14 November 2019.

This paper was selected for presentation by an SPE program committee following review of information contained in an abstract submitted by the author(s). Contents of the paper have not been reviewed by the Society of Petroleum Engineers and are subject to correction by the author(s). The material does not necessarily reflect any position of the Society of Petroleum Engineers, its officers, or members. Electronic reproduction, distribution, or storage of any part of this paper without the written consent of the Society of Petroleum Engineers is prohibited. Permission to reproduce in print is restricted to an abstract of not more than 300 words; illustrations may not be copied. The abstract must contain conspicuous acknowledgment of SPE copyright.

Abstract

Correctly evaluating reservoirs with thin laminations can be challenging. From a conventional perspective, this type of reservoir is often considered to be nonpay because of its low resistivity. Tensor models help improve resistivity using horizontal (R_H) and vertical (R_V) resistivity measurements from triaxial induction logging tools. In the absence of triaxial advanced measurements of R_H and R_V , tensor model equations using a conventional openhole (triple combo data) can be used.

This approach is based on rearranging the tensor model with the Moran-Gianzero equation and using several assumptions for unique cases. This method explains the workflow to calculate sand resistivity correctly using only openhole data as well as calculating the anisotropic shale resistivity that is often estimated from nearby shales. A mathematical method is preferred to obtain consistent results for anisotropic shale resistivity parameters to reduce calculation uncertainty. Sensitivity analyses are created to provide a sense of how these parameters affect the results on sand resistivity.

For a vertical well where relative dip is close to zero, R_{Sd} can be calculated without knowing the R_{shV} . The same equation provides a 10% error on R_{Sd} at $V_{Lam} < 10\%$ and relative dip $< 10^\circ$. At a higher relative dip and anisotropic shale resistivity, a cubic equation with a new coefficient is proposed. Sensitivity analyses are made to compare a true R_{Sd} and calculated R_{Sd} with changing R_{shH} and R_{shV} variables. The model demonstrates that a 10% change on R_{shH} could cause a 30% error on R_{Sd} at V_{Lam} of 10%, while changes in R_{shV} only begins to affect R_{Sd} up to 30% at V_{Lam} 70%. Graphical and mathematical methods are proposed to help prevent misestimating the R_{shH} and R_{shV} . The graphical method is preferred when a complete data set for all relative dip is available, while the mathematical method is preferred when the data set is limited.

Unique cases where the R_{Sd} can be calculated as well as demonstrations on how anisotropic shale resistivity parameters can be determined using only conventional openhole (triple combo) data are highlighted. The additional set of constraints on the iteration of the cubic equation represents an improvement of the previous study, whereas the proposed method to determine the R_{shH} and R_{shV} helps prevent estimation errors of these parameters and helps improve R_{Sd} calculation accuracy.

Introduction

The laminated sand-shale reservoir is common in many siliciclastic depositional environments—from deepwater to aeolian (Passey et al. 2006)—and approximately 30% of global hydrocarbon reserves come

from this type of reservoir (Mollison et al. 2001). A good understanding of laminated sand-shales reservoirs could be important to maximize the hydrocarbon potential of this play.

Laminated Sand-Shale Reservoir

Different from the sedimentology definition, a lamination in petrophysics is defined as a thickness less than the tool vertical resolution (typically 2 ft and less). Under that condition, a laminated sand-shale reservoir can introduce an electrical anisotropy effect that can make the conventional resistivity read too low. Evaluating a laminated sand-shale reservoir using a conventional method always calculates a high water saturation, registering the reservoir as nonpay. The fact that some of this type of reservoir often produces a high amount of hydrocarbon with little or no water produced means that a different approach is necessary.

Addressing this challenge has been attempted for several decades, dating back to 1933 by Conrad Schlumberger. Yin et al. (2008) provided an overview for these models before 2008. All models typically introduce sand resistivity (R_{sd}) as an improved version of conventional low resistivity. In general, the equation usually incorporates vertical resistivity (R_v) and horizontal resistivity (R_H) measurements from an advanced triaxial induction tool to calculate the R_{sd} . In the absence of such an advanced measurement, a tensor model can be used with conventional openhole data. However, this technique requires that anisotropic shale resistivity parameters (R_{shH} , R_{shV}) are known. Incorrect or misestimated values can introduce an error for the R_{sd} calculation. This study reviews the tensor model by using conventional openhole data and demonstrates how anisotropic shale resistivity parameters can be determined to reduce uncertainty on R_{sd} calculations.

Resistivity Anisotropy

There are two types of resistivity anisotropy: macroscopic anisotropy, caused by the inability of the conventional resistivity tool to measure the true resistivity of an individual thin layer less than the vertical resolution of the tool, and microscopic anisotropy, caused by intrinsic formation properties (e.g., a stratified grain of sand in a rock or elongated mica minerals in shales).

For a laminated sand-shale reservoir, alternating between typically higher sand resistivity and lower shale resistivity causes a macroscopic anisotropy effect on conventional resistivity measurements. For a vertical well (relative dip close to zero) with anisotropic shale, resistivity can have two components on the electrical measurement, depending on its direction. An electric measurement parallel to the lamination that acts as a parallel resistor circuit is the R_H (Fig. 1).

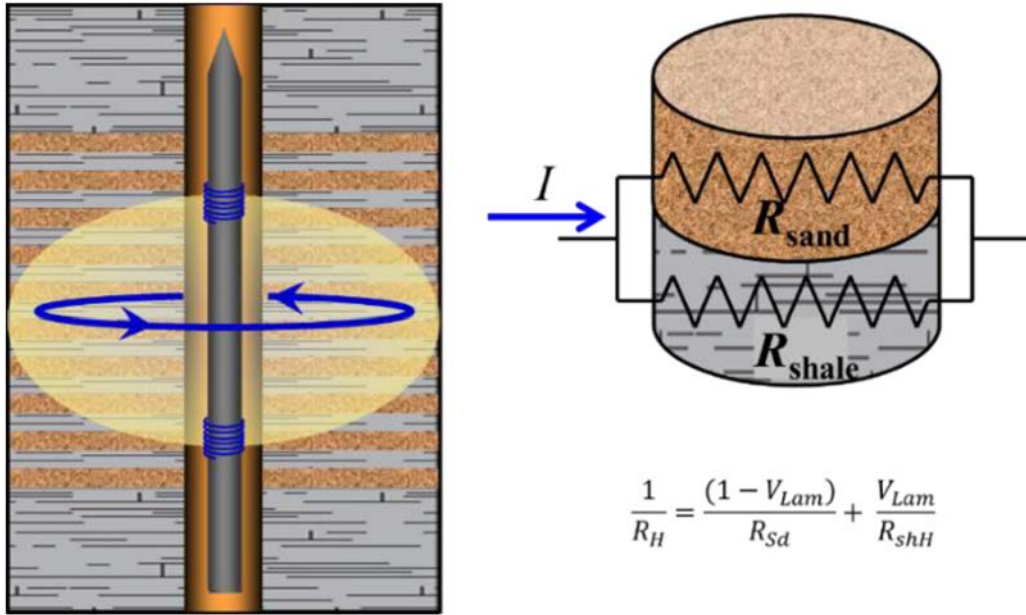


Figure 1—Parallel resistivity measurement of sand-shale lamination.

An electric measurement perpendicular to the lamination that acts as a series resistor circuit is the R_V (Fig. 2).

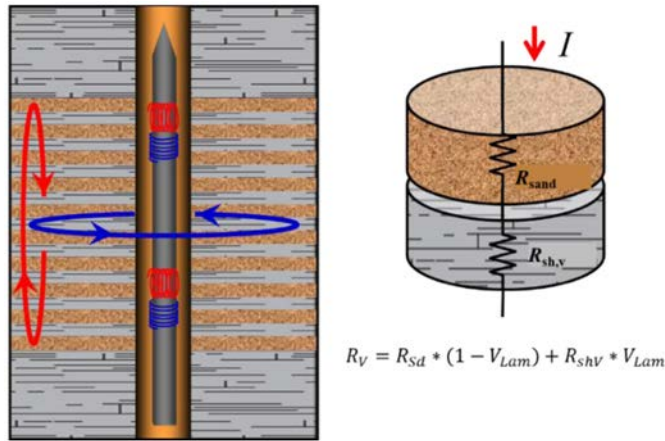


Figure 2—Perpendicular resistivity measurement of sand-shale lamination.

These two components are part of the tensor model equation, and each is a function of the laminated shale volume (V_{Lam}), sand resistivity (R_{Sd}), and anisotropic vertical and horizontal shale resistivity (R_{shV} , R_{shH}) (Eqs. 1 and 2).

$$\frac{1}{R_h} = \frac{(1 - V_{Lam})}{R_{Sd}} + \frac{V_{Lam}}{R_{shH}} \tag{1}$$

$$R_V = R_{Sd} * (1 - V_{Lam}) + R_{shV} * V_{Lam} \tag{2}$$

Another important equation (Eq. 3) (Moran and Gianzero 1979) demonstrates that a resistivity measurement (R_{Log}) from a conventional resistivity tool is a result of R_V , R_H , and α (relative dip/angle between bedding dip and borehole inclination).

$$R_{Log} = \frac{\lambda R_H}{\sqrt{\sin^2\alpha + \lambda^2 * \cos^2\alpha}} ; \lambda^2 = \frac{R_V}{R_H} \tag{3}$$

When other parameters are constant, the bigger the relative dip (α), the higher the conventional resistivity log (R_{Log}) (Fig. 3). Together with the tensor model equations, Eqs. 1, 2, and 3 govern the resistivity behavior for laminated sand-shale reservoirs, and they can be used to calculate the R_{Sd} from openhole data.

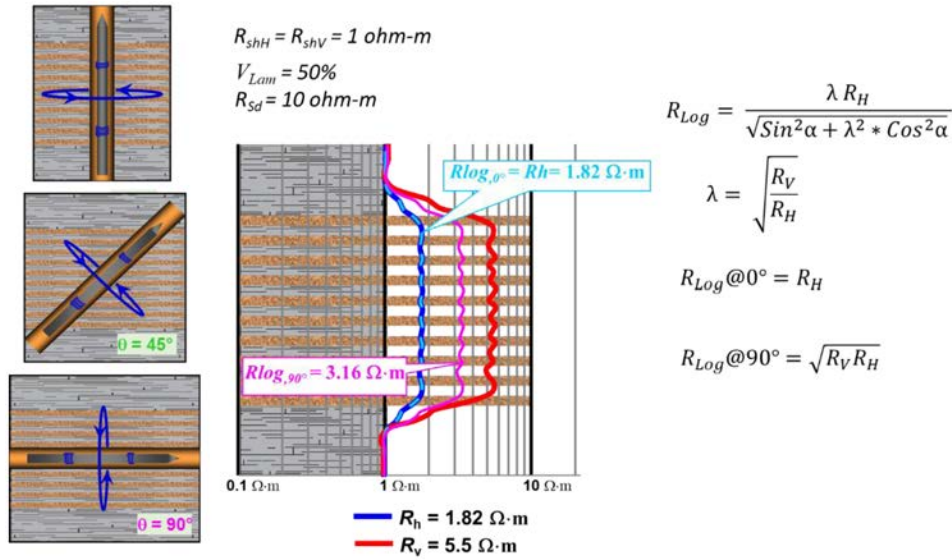


Figure 3—Relative dip (α) effect on R_{Log} measurement.

Openhole Tensor Model ($\alpha \sim 0$)

For a vertical well with a horizontal bedding dip ($\alpha \sim 0$), R_{Sd} can be calculated using only R_{Log} conventional resistivity data and V_{Lam} from a Thomas-Stieber plot. At zero α , Eq. 4 proves that R_{Log} is always equal to R_H ; thus, R_{shH} could be determined from R_{Log} at the thick shale section. It is assumed that shale properties at the laminated sand-shale are the same as the thick shale interval.

$$R_{Log} = \frac{\lambda R_H}{\sqrt{\sin^2 \alpha + \lambda^2 \cos^2 \alpha}} = \frac{\lambda R_H}{\sqrt{\sin(0^\circ)^2 + \lambda^2 \cos(0^\circ)^2}}$$

$$R_{Log} = \frac{\lambda R_H}{\sqrt{(0)^2 + \lambda^2 (1)^2}} = \frac{\lambda R_H}{\sqrt{\lambda^2}} = R_H \quad (4)$$

$$R_{Log} = R_H; \quad R_{Log} \text{ at thick shale} = R_{shH}$$

Using Eq. 4, the R_{Sd} can be calculated using Eq. 5:

$$\frac{1}{R_h} = \frac{(1-V_{Lam})}{R_{Sd}} + \frac{V_{Lam}}{R_{shH}}, \quad \frac{1}{R_{Log}} = \frac{(1-V_{Lam})}{R_{Sd}} + \frac{V_{Lam}}{R_{shH}}$$

$$\frac{(1-V_{Lam})}{R_{Sd}} = \frac{1}{R_{Log}} - \frac{V_{Lam}}{R_{shH}}, \quad \frac{(1-V_{Lam})}{R_{Sd}} = \frac{R_{shH} - (R_{Log} * V_{Lam})}{R_{Log} * R_{shH}} \quad (5)$$

$$R_{Sd} = \frac{(1-V_{Lam}) * R_{Log} * R_{shH}}{R_{shH} - (R_{Log} * V_{Lam})}$$

Using Eq. 5, R_{Sd} can be calculated using V_{Lam} , R_{Log} , and R_{shH} . For a well with a relative dip of zero, the vertical component of resistivity (i.e., R_{shV} , R_V) does not affect the R_{Sd} calculation result. For conditions where the relative dip is not zero, this equation still can be used with an error in mind. Using Eq. 5, a model of constant R_{shV} , R_{shH} , and R_{Sd} is produced (Fig. 4) (R_{Sd} is set to be 30 ohm-m). The model demonstrates that the calculated R_{Sd} has different error rate percentages with changing V_{Lam} and α . This error percentage is governed by the ratio of R_{Sd} and R_{shH} .

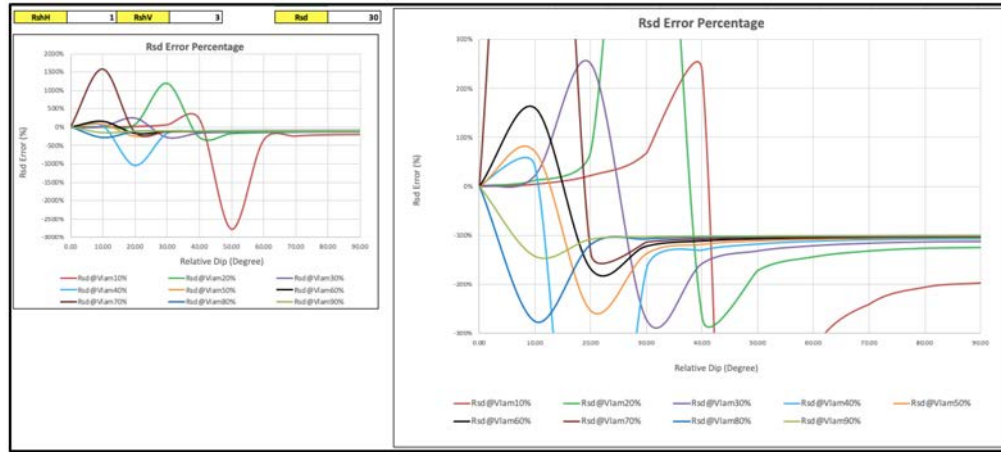


Figure 4— R_{sd} error percentage over changing V_{Lam} and α (R_{sd} set to be 30 ohm-m).

Interpretation-wise, this model could be used to see how far (error percentage) the calculated R_{sd} could deviate from the true R_{sd} if the relative dip is greater than zero. For example, a R_{shH} of 1 ohm-m and R_{sd} of 30 ohm-m at V_{Lam} 10% and α of 10° calculates R_{sd} 5% higher than its true value. It is safe to say that a $V_{Lam} < 10\%$ and $\alpha < 10^\circ$ calculates R_{sd} with errors less than 10% from its true value. Although calculating R_{sd} using Eq. 5 is possible when the relative dip is 10° and less, anything higher produces errors greater than 10% (particularly when $V_{Lam} > 30\%$). Another method to calculate R_{sd} is necessary.

Openhole Tensor Model ($\alpha > 0$)

At higher relative dip, vertical components start affecting the calculated R_{sd} result (Fig. 4), and the tensor model Eqs. 1 and 2 should be used to calculate R_{sd} to account for the vertical component of resistivity. Calculations using tensor model Eqs. 1 and 2 require multiple inputs to be known (i.e., R_H , R_V , V_{Lam} , R_{shH} , and R_{shV}). Out of the five inputs, only two are usually known from conventional openhole data, such as V_{Lam} (Thomas-Stieber) and R_{shH} ; the other remaining three inputs are not available from conventional openhole data.

The workaround for this is a method (Fylling 1991) to calculate R_{sd} in a form of C_{sd} by combining tensor model Eqs. 1 and 2 and Moran-Gianzero Eq. 3, assuming an isotropic shale ($R_{shH}=R_{shV}=R_{sh}$). The solution is rewritten in a form of R_{sd} as follows:

$$\frac{a_1}{R_{sd}^3} + \frac{a_2}{R_{sd}^2} + \frac{a_3}{R_{sd}} + a_4 = 0 \quad (6)$$

with a_n as follows:

$$a_1 = \frac{V_{Lam} * (1 - V_{Lam})^2 * \cos^2 \alpha}{R_{sh}^2} \quad (7)$$

$$a_2 = \frac{(1 - V_{Lam}) * (1 + V_{Lam} * (3V_{Lam} - 2)) * \cos^2 \alpha}{R_{sh}^3} \quad (8)$$

$$a_3 = \frac{V_{Lam} * ((1 + (1 - 4V_{Lam} + 3V_{Lam}^2)) * \cos^2 \alpha)}{R_{sh}^2 - R_{Log}^2} \quad (9)$$

$$a_4 = \frac{(1 - V_{Lam}) * V_{Lam}^2 \cos^2 \alpha}{R_{sh} R_{Log}} \quad (10)$$

Using Eq. 6, the R_{sd} can be calculated using known input parameters (V_{Lam} , R_{Log} , R_{sh} , R_{Log} , α) from conventional openhole data. The positive root from this equation is the R_{sd} value; however, Eq. 6 assumes

the shale is isotropic, even though most of the time the shale is anisotropic. When the shale is anisotropic ($R_{shH} \neq R_{shV}$), Eq. 6 is no longer valid. The error can be up to greater than 30% (Fig. 5).

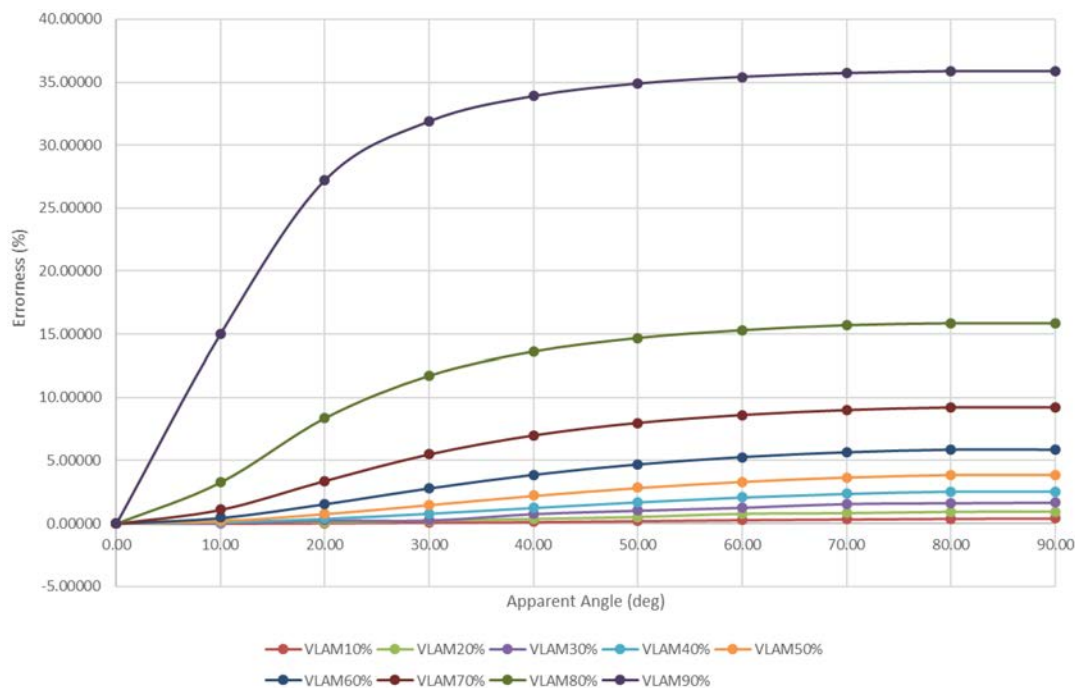


Figure 5— R_{sd} error percentage using isotropic shale cubic equation method

Under the same approach, the author produced an additional set of constraints and iteration processes for the cubic equation solution for R_{sd} compared to the previously mentioned author.

Fig. 6 shows the iteration workflow. The step-by-step process is as follows:

1. Calculate the R_{sd} by assuming the shale is isotropic using Eq. 6.
2. With the calculated R_{sd} from Step 1, calculate R_v and R_H using the tensor model Eqs. 1 and 2.
3. With the calculated R_v and R_H from Step 2, back-calculate R_{Log} using Moran-Gianzero Eq. 3, which now becomes R_{Log}' .
4. Compare it to the R_{Log} from conventional openhole data; the difference between these two ($R_{Log}' - R_{Log}$) should be minimum.
5. If the difference is not close to zero, change R_{sd} and repeat Step 3 until the difference is minimized.

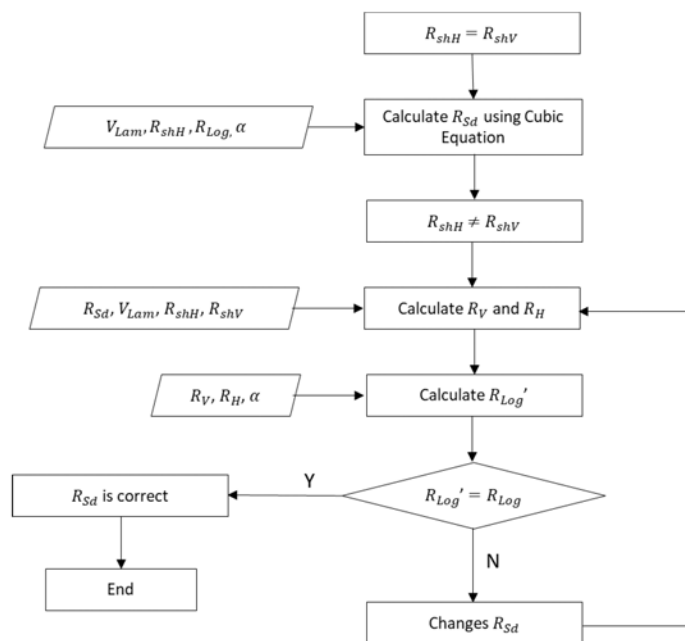


Figure 6—Iterative process to calculate R_{sd} in a high relative dip.

Anisotropic Shale Resistivity

The workflow to calculate R_{sd} explained in Fig. 5 is based on the assumption of the value of anisotropic shale resistivity (i.e., R_{shV} and R_{shH}); this is where the calculation error of R_{sd} could occur. The best practice for R_{shH} value is usually taken from the conventional resistivity log (R_{Log}) at a shale section where the amount of V_{Lam} is at maximum (or close to 100%). However, R_{Log} at 100% V_{Lam} could be different with R_{shH} when the relative dip is not zero. Fig. 7 shows a variation on R_{Log} value at 100% V_{Lam} with relative dip changes.

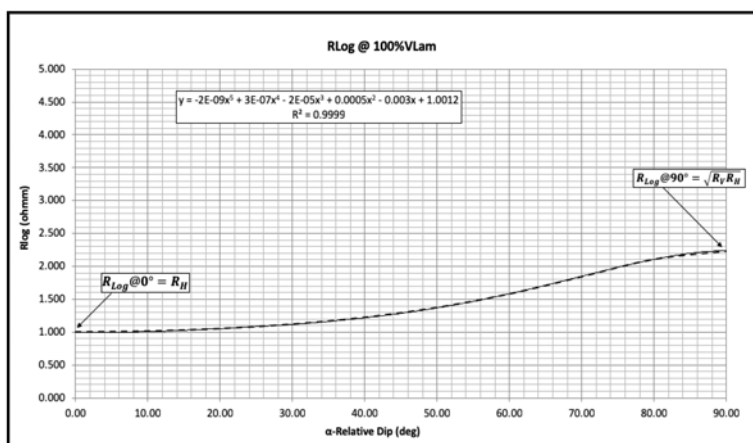


Figure 7—Polynomial Order 5 relationship between R_{Log} and relative dip.

The relationship between R_{Log} and V_{Lam} is Polynomial Order 5. One should correct for the relative dip to get the true R_{shH} from conventional log data. When data is limited, a graphical solution to calculate the true R_{shH} and R_{shV} can be performed. However, the accuracy on R_{shV} depends heavily on available data at a higher relative dip because Polynomial Order 5 requires more data to be correct. If available data is only at an approximate relative dip of 45° or less, the regression is in Polynomial Order 3 instead of 5 (Fig. 8) because the extrapolation to 90° is less than what it should be for Polynomial Order 5.

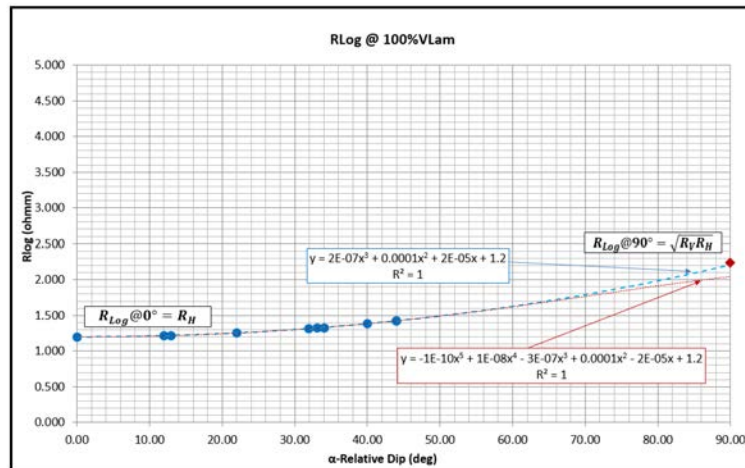


Figure 8—Polynomial Order 3 relationship at available data lower than 45°.

Between the two, R_{shH} is the most important parameter in the tensor model; a small change of R_{shH} can cause a big error in R_{Sd} (Fig. 9). The model is built based on 50-ohm-m R_{Sd} , 1.1-ohm-m R_{shH} , and 5-ohm-m R_{shV} . The error percentage comes from changing the R_{shH} 10% higher than its true value [i.e., 1.1 ohm-m of R_{shH} (other parameters remain unchanged)]. As can be observed, even a 10% error higher on R_{shH} at 10% V_{Lam} and 30° α could cause a 30% error lower on calculated R_{Sd} .

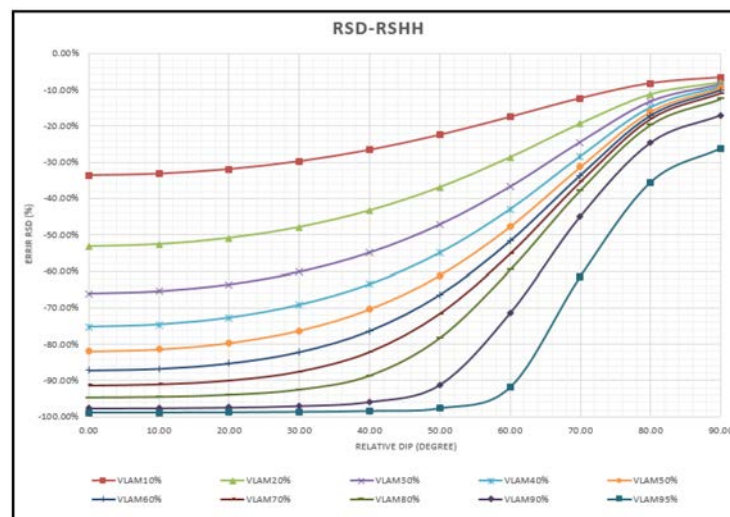


Figure 9— R_{Sd} error analysis with changing variable of R_{shH} .

As for R_{shV} , it usually requires an educated guess on the anisotropy ratio between R_{shV} and R_{shH} ; the number is usually approximately two to three times more than R_{shH} ($R_{shV} = 2\sim 3 \cdot R_{shH}$). This assumption usually works during a situation where the amount of laminated shale volume (V_{Lam}) is small, then the impact on calculated R_{Sd} would be small. According to the model (50 ohm-m R_{Sd} , 1 ohm-m R_{shH} , and 3 ohm-m R_{shV}), using a wrong R_{shV} (3 ohm-m instead of 5 ohm-m) results in an R_{Sd} error of less than 10% when the V_{Lam} is 70% or less. Greater than that, the R_{Sd} error would increase to more than 10% to as high as 75% greater than its R_{Sd} value should be (Fig. 10). The focus should be placed on attaining the correct R_{shH} before going to R_{shV} because the small changes on R_{shH} impact R_{Sd} the most compared to R_{shV} .

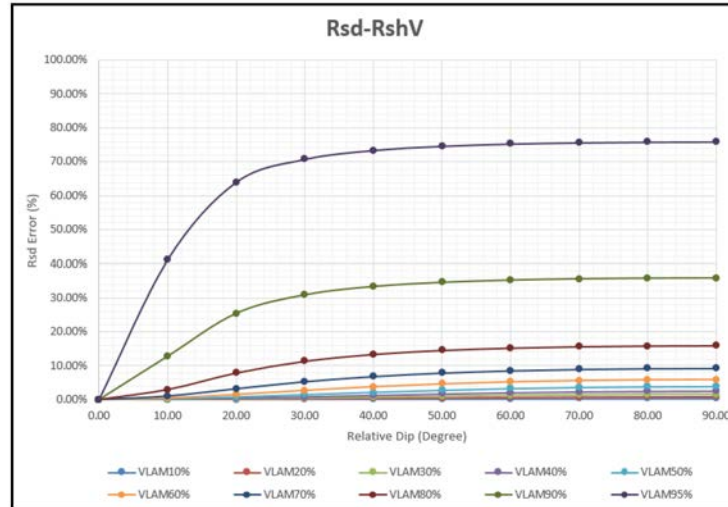


Figure 10— R_{sd} error analysis with changing variable of R_{shV} .

R_{shH} and R_{shV} Determination

Because the anisotropic shale resistivity (R_{shH} and R_{shV}) is the most important parameter in the tensor model, the author proposes a mathematical method to determine its value based on the conventional log. This technique does not require data like the graphical method previously mentioned. This method is based on the substitution method that uses a minimum of two sets of data on different R_{Log} and α -relative dip at 100% V_{Lam} depth. The equation is as follows:

$$A + BX_1 - X_1 * X_2 = 0 \quad (11)$$

where A, B, X_1 , X_2 are

$$A = R_{Log}^2 * \sin^2 \alpha \quad (12)$$

$$B = R_{Log}^2 * \cos^2 \alpha \quad (13)$$

$$X_1 = \frac{R_{shV}}{R_{shH}} \quad (14)$$

$$X_2 = R_{shH}^2 \quad (15)$$

With two data sets, the first set of R_{Log} and α is marked as A_1 - B_1 , and the second set is A_2 - B_2 . Then rearranging Eq. 11 produces

$$X_1 = \frac{A_1 - A_2}{B_1 - B_2} = \frac{R_{shV}}{R_{shH}} \quad (16)$$

Once X_1 is calculated, use either Eq. 1 or Eq. 2 to calculate X_2 using Eq. 17:

$$X_2 = \frac{A_1 + BX_1}{X_1} = R_{shH}^2 \quad (17)$$

Fig. 11 shows an example of the preceding equation.

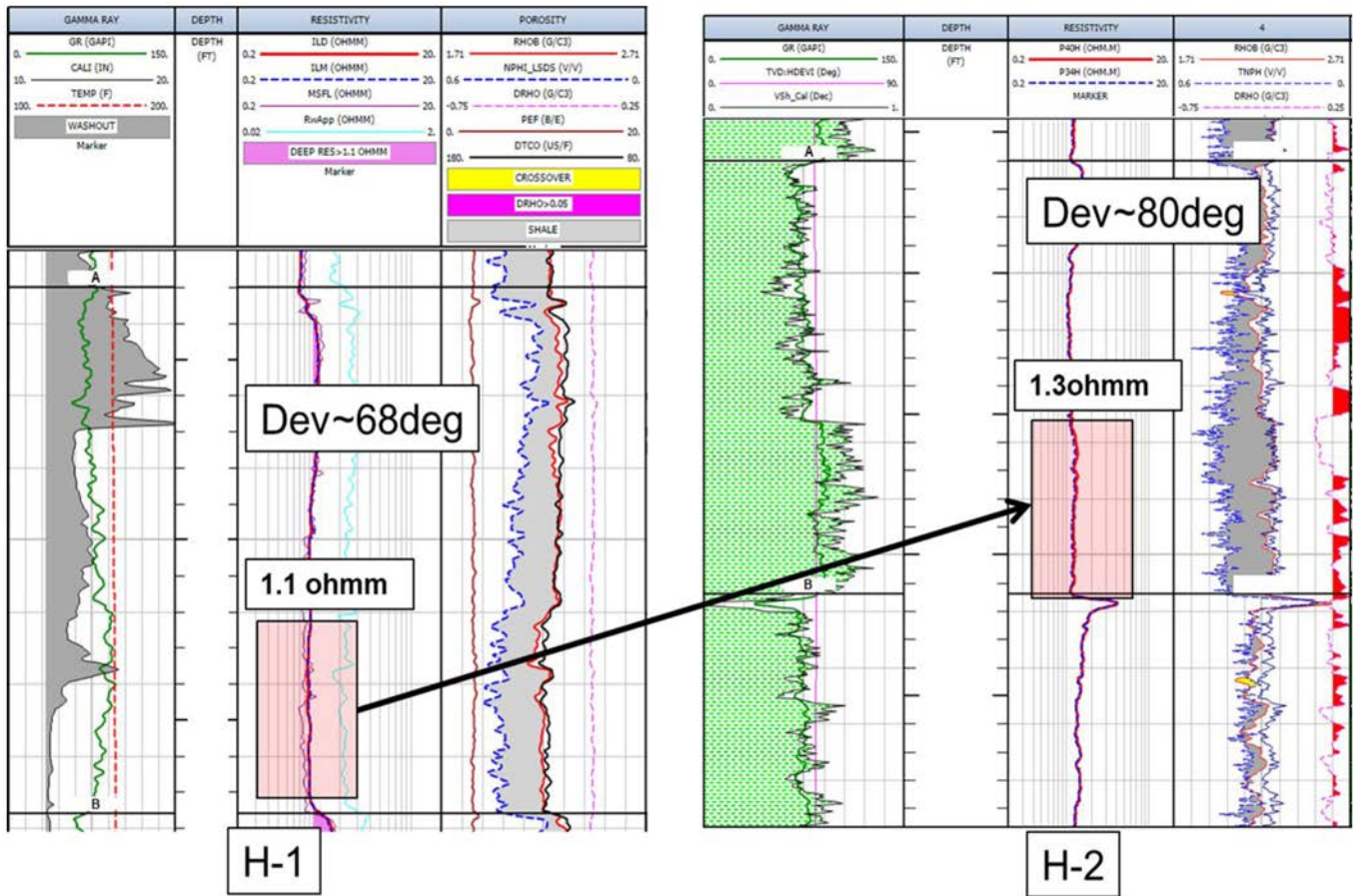


Figure 11—Explanation of the equation.

For the first dataset from Well H-1, Eq. 11 produces

$$\begin{aligned} A_1 + B_1 X_1 - X_1 * X_2 &= 0 \\ 1.04 + 0.169 X_1 - X_1 * X_2 &= 0 \end{aligned} \quad (18)$$

while the second dataset from Well H-2 produces

$$\begin{aligned} A_2 + B_2 X_1 - X_1 * X_2 &= 0 \\ 1.639 + 0.051 X_1 - X_1 * X_2 &= 0 \end{aligned} \quad (19)$$

Combining both Eqs. 18 and 19 in a form of X_1 and X_2 through elimination or substitution produces

$$X_1 = \frac{R_{shV}}{R_{shH}} = 0.1984; \quad X_2 = R_{shH}^2 = 0.3762 \quad (20)$$

Therefore, the true RshH and RshV is RshH = 0.61 ohm-m, while $R_{shV} = 3.09$ ohm-m. Assuming R_{shH} and R_{shV} where the R_{Log} and α -relative dip were taken is not changing, this method can easily calculate both R_{shH} and R_{shV} from conventional log data, reducing the uncertainty that could cause errors when calculating R_{sd} using the tensor model.

Conclusions

The tensor model and Moran-Gianzero equations are combined to calculate R_{sd} from conventional openhole data. For cases where the relative dip is approximately 0° , a simple equation can be used to calculate R_{sd} without knowing the R_{shV} . Additionally, it can be used at higher relative dip up to 10° with $<10\%$ error on calculated R_{sd} .

At higher relative dip and anisotropic shale resistivity, the cubic equation published by Fylling (1991) calculates the wrong R_{Sd} . The author proposes an additional constraint and iteration process to the cubic equation, which helps improve the calculation process and provides the correct R_{Sd} . The iteration process relies on the R_{shH} and R_{shV} parameters, particularly R_{shH} . A sensitivity analysis demonstrates that a 10% change on R_{shH} could cause a 30% error on R_{Sd} at V_{Lam} of 10%, while changes in R_{shV} only begin to affect R_{Sd} up to 30% at V_{Lam} 70%.

Graphical and mathematical methods are proposed to help prevent misestimating the R_{shH} and R_{shV} . The graphical method is preferred when a complete data set for all relative dip is available, while the mathematical method is preferred when the data set is limited.

Acknowledgements

The author thanks Halliburton for full support publishing this study.

References

- Fylling, A. 1991, Estimating Conductivity and Saturations in the Sands of Thinly Laminated, Dipping Sand/Shale Sequences. Presented at the SPWLA 32nd Annual Logging Symposium, Midland, Texas, 16–19 June. SPWLA-1991-O.
- Hagiwara, T. 1997. "Macroscopic Anisotropy" Approach to Analysis of Thinly Laminated Sand/Shale Sequences: Sensitivity Analysis of Sand Resistivity Estimate and Environmental Corrections. Presented at the SPE Annual Technical Conference and Exhibition, San Antonio, Texas, 5–8 October. SPE-38669-MS. <https://doi.org/10.2118/38669-MS>.
- Kyi, K. K., Wang, A. G. J., Quirein, J. et al 2014. Minimizing the Uncertainty in Laminated Shaly Sand Evaluation Using Nuclear MCI-NMR-OMRI Technologies: A Case Study in Offshore Terengganu, Malay Basin. Presented at the Offshore Technology Conference-Asia, Kuala Lumpur, Malaysia, 25–28 March. OTC-25038-MS. <https://doi.org/10.4043/25038-MS>.
- Mollison, R. A., Fannini, O. N., Kriegshauser, L. et al 2001. Impact of Multicomponent Induction Technology on a Deepwater Turbidite Sand Hydrocarbon Saturation Evaluation. Presented at the SPWLA 42nd Annual Logging Symposium, Houston, Texas, 17–20 June. SPWLA-2001-T.
- Moran, J. H. and Gianzero, S. C. 1979. Effects of formation anisotropy on resistivity measurements. *Geophysics*, **44**(7): 1266–1286. <https://doi.org/10.1190/1.1441006>.
- Passey, Q. R., Dahlberg, K. F., Sullivan, K. B. et al 2006. Petrophysical Evaluation of Hydrocarbon Pore-Thickness in Thinly Bedded Clastic Reservoirs. *AAPG Archie Series*, No. 1. <https://doi.org/10.1306/A11157>.